Modelling long term basin scale sediment connectivity, driven by spatial land use changes

Tom J. Coulthard[1*] and Marco J. Van De Wiel[2]

[1] Department of Geography, Environment and Earth Science, University of Hull, Hull, UK

[2] Centre for Agroecology Water and Resilience, Coventry University, Coventry, UK

[*] T.Coulthard@hull.ac.uk

Abstract

Changes in land use can affect local geomorphology and sediment dynamics. However, these impacts could conceivably lead to changes in geomorphological processes beyond the area of land use change, thereby evidencing a geomorphic connectivity in the landscape. We conduct a numerical modelling experiment, using the CAESAR landscape evolution model, to investigate the extent and nature of such connectivity in the River Swale basin. Six simulations are run and analysed. Two of these are reference simulations, where the basin has a hypothetical total grassland cover or total forest cover. In the other four simulations, half of the basin is subjected to either deforestation or reforestation during the simulation. Simulations are analysed for temporal trends in sediment yield and for spatial trends in erosion and deposition across the basin. Results show that deforestation or reforestation in one half of the basin can indeed affect the geomorphology of the other half, thus implying a geomorphological connectivity across the basin. This connectivity is locally very high, with significant morphological impacts close to where de- or re-forestation occurs. Changes are observed both downstream and upstream of the areas where the land use changes occurred. The impacts are more pronounced in the downstream direction and are still apparent in the basin scale sediment yields, as deforestation of half the basin can increase decadal sediment yields by over 100%, while reforestation of half the basin can lead to 40% decreases. However, our results also indicate a *reverse connectivity* whereby erosion and deposition in upstream headwaters and tributaries can, for the first time, be conclusively attributed to land use changes several kilometres downstream, due to alterations in the valley floor base level resulting from incision and alluviation.

1. Introduction

Land use changes within basins can clearly have a significant impact on sediment dynamics and therefore basin connectivity. Over recent time scales changes including deforestation (Marden et al., 2005; Ward et al., 2009) as well as reforestation (Hooke, 2006; Keesstra et al., 2009; Liébault et al., 2005) have been shown to alter sediment movement and basin connectivity. Looking to longer Holocene and Quaternary scales, there have been many studies looking at how the fluvial response to land use changes (as well as climate) are reflected in the alluvial archive. That is, how environmental change may lead to periods of alluviation (deposition), incision and channel pattern change (e.g. Brown, 2002; Macklin et al., 2012, 2005).

The debate surrounding the causes of changes in Holocene river behaviour and alluvial archives is ongoing and has at times been polarised. Initial studies suggested that changes in land use such as widespread deforestation and the adoption and developments in agriculture were responsible for transforming river behaviour and alluvial environments (Brown and Barber, 1985; Burrin, 1985). Further to this, work across Northern Europe indicated that changes in alluviation appeared to coincide with the growth of human population across Europe due to increased soil erosion rates from agricultural practices (Bork and Lang, 2003; Dotterweich, 2008; Houben, 2008; Lang, 2003). For the UK, Ballantyne (1991) summarised that late Holocene forest clearance and increased grazing pressures led to increased solifluction, vegetation stripping and soil erosion. In the Howgill fells of NW England, Harvey and Renwick, (1987) linked changes in alluvial fan accumulation and dissection pre 2000 BP and post 1000 BP with regional settlement expansions, implying a link to deforestation. Continuing from this, Harvey (1996) suggested that widespread gulley development in the same area were due to changes in basin hydrology caused by deforestation. He also suggested that steep upland systems (like the Howgills) may be gemorphologically sensitive to such land use/hydrological changes.

However, as both the number of dated alluvial records and their geographical spread increased it became apparent that changes in alluviation were occurring at similar times in many locations across countries and Europe. This led to an alternative theory that the dominant control was climate – as only large scale shifts in weather patterns could cause such a widespread changes (Macklin and Lewin, 2003, 1993; Macklin et al., 1992). As the debate matured, it became clear that both land use and climate change could and were exerting controls over Holocene river alluviation and behaviour, with Macklin et al. (1992) using the term "*climatically driven but culturally blurred*". Most recently, with the emergence of the Anthropocene, the importance of land use change in certain locations has been further re-enforced (Macklin et al., 2014, 2010)

Many of the studies cited above pre-date the widespread use of the term connectivity, including the work of Harvey, (1991, 2002, 2001) who first used the term coupling to describe the linkages between hillslopes and channels. These and the previously cited studies are all demonstrating the components of connectivity as later outlined by Bracken and Croke (2007). For example, how changes in external and internal parameters affect basin morphology, sediment yield and stratigraphy. Fryirs et al.'s (2007) sediment buffers, barriers and blankets are all facets of how a drainage basin processes sediment delivery. Indeed, recent publications have acknowledged the overlap of the long term fluvial studies and connectivity (Baartman et al., 2013; Macklin et al., 2014).

One question that has proved hard to answer, is what are the *relative* roles of climate and land use in affecting fluvial behaviour? This question is especially important for researchers wishing to invert the alluvial record (e.g. a terrace sequence or a stratigraphy) to calculate past climate and/or land use changes. This process is significantly complicated by the possibility that climate and land use can change at the same time.

Numerical modelling has been used to directly address this research question, with early work using the CAESAR Landscape Evolution Model looking at the relative importance of climate and land use change on basin sediment yield (Coulthard et al., 2000). Modelling a small basin in the Yorkshire Dales, UK, this research showed how decreasing tree cover *or* increasing rainfall magnitudes resulted in a 25-100% increase in simulated sediment yield – whereas changing both together let do a 1300% increase (Coulthard et al., 2000). Whilst it is impossible to validate these percentage changes, the sharp difference in basin responses suggested that whilst climate was the main driver, land use changes primed the basin to respond (Coulthard et al., 2000). Over longer time scales (9000 years) and on a much larger basin, a similar effect was observed, with changes in simulated sediment yields being amplified by a reduced tree cover (Coulthard and Macklin, 2001). The CAESAR model was also used by Welsh et al. (2009) with a temporally varying land use – examining how changes in land use during the last 500 years affected sediment yields from the Alpine basin of Petit Lac de Annecy, France. However, in all of these studies both climate and land use changes were lumped over the whole basin.

Numerical models have also been used to look at connectivity both directly and indirectly. Researchers have looked at how connectivity is effected by vegetation, morphology and the role of humans (Lexartza-Artza and Wainwright, 2009; Michaelides and Chappell, 2009; Wainwright et al., 2011) with Baartman et al. (2013) using the LAPSUS model to show how valley and catchment shape impacts on sediment connectivity. Indirectly, (not mentioning connectivity specifically) there is a growing body of research examining how environmental ‘signals’ propagate through systems and

how the internal operation of a drainage basin can generate its own or *autogenic* signals. Jerolmack and Paola (2010) suggested that environmental systems, including drainage basins, can act as signal 'shredders'. Based on physical models (a flume model and a rice pile) they showed how variations to the model inputs were not replicated in the outputs with the internal storage and release of sediment and rice within the models (the autogenic processes) masking or shredding the input signal. Only very large changes to the sediment input that were greater than the size of the system were capable of being replicated in the outputs. In related research, Castelltort and Van Den Driessche (2003) and Simpson and Castelltort (2012) showed how a numerical model of a river floodplain could buffer or remove any signals from changing sediment inputs. Coulthard and Van de Wiel (2013) modelled how tectonic and climate signals were transmitted through a drainage basin, indicating that whilst climate changes were reflected in increases in sediment yield rapidly, increases in upstream erosion due to tectonic uplift were buffered and not transmitted downstream by even a short length of floodplain. Coulthard and Van De Wiel (2007), Coulthard et al. (2005) and Van De Wiel and Coulthard (2010) looked at how the autogenic processes within a drainage basin can generate spikes in sediment outputs even with constant forcings, suggesting that linking cause (climate or land use change) to effect (alluviation) may be impossible in certain circumstances.

Therefore, the existing body of modelling research on basin connectivity has provided us with important insights into how climate and tectonic signals propagate through drainage basins as well as how autogenic factors are highly important. However, within all of these studies there has been no consideration on how spatial changes in land use over time have an impact on basin connectivity and sediment yield. One of the most significant causes of land use change is deforestation – but how does the spatial pattern, or manner of this change affect patterns of erosion and deposition, sediment connectivity and sediment yield? For example, will deforestation from uplands to lowlands give a different response to deforestation from lowlands to uplands?

This paper aims to answer these questions by modifying the CAESAR-Lisflood numerical model (Coulthard et al., 2013) to simulate how spatial and temporal changes in land use (e.g. deforestation) affect erosion and deposition in a large drainage basin over centennial time scales. The following sections describe the modifications made to the model to make this possible, the field study area and the land use/deforestation scenarios we chose to investigate.

2. Methods

2.1 Modifications to the CAESAR-Lisflood model

CAESAR-Lisflood is a raster based Landscape Evolution Model (LEM) using a hydrological model to generate spatially distributed runoff, that is then routed using a quasi 2D hydrodynamic model generating flow depths and velocities. These depths and velocities are then used to calculate fluvial erosion and deposition for up to nine different grainsizes integrated within an active layer system. Furthermore, slope processes (mass movement and soil creep) are also included in the simulations and a full description of CAESAR-Lisflood is provided in Coulthard et al., (2013) and Van De Wiel et al., (2007). Most previous applications of CAESAR-Lisflood had used a lumped hydrological model based on TOPMODEL (Beven and Kirkby, 1979) where the *m* value that controls the rate of rise and decay of the hydrograph was kept constant over the whole basin. As described in the introduction, some studies had altered *m* over the whole basin to represent changing basin land use (e.g. Coulthard and Macklin, 2001; Welsh et al., 2009) but none had looked at spatial variations therefore requiring modifications to CAESAR-Lisflood to allow both temporal and spatial changes in the hydrological model. A detailed description of the revised hydrological model within CAESAR-Lisflood is provided below, but for more detail of the hydraulic, fluvial erosion and slope model operation readers are referred to Coulthard et al., (2013a).

The hydrological model within CAESAR-Lisflood is an adaptation of TOPMODEL (Beven and Kirkby, 1979) containing an area lumped exponential store of water where storage and release of water is controlled by the m parameter (Equations 1 and 2).

If the local rainfall rate r (m h^{-1}) specified by an input file is greater than 0, the total surface and subsurface discharge (Q_{tot}) is calculated using equation (1).

Equation 1.

$$Q_{tot} = \frac{m}{T}\log\left(\frac{(r - j_t) + j_t \exp\left(\frac{rT}{m}\right)}{r}\right)$$

$$j_t = \frac{r}{\left(\frac{r - j_{t-1}}{j_{t-1}}\exp\left(\left(\frac{(0 - r)T}{m}\right) + 1\right)\right)}$$

Here, T = time (seconds); j_t = soil moisture store; j_{t-1} = soil moisture store from the previous iteration. If the local rainfall rate r is zero (i.e. no precipitation during that iteration), equation (2) is used:

Equation 2.

$$Q_{tot} = \frac{m}{T}\log\left(1 + \left(\frac{j_t T}{m}\right)\right)$$

$$j_t = \frac{j_{t-1}}{1 + \left(\frac{j_{t-1} T}{m}\right)}$$

In Equations 1 and 2, m controls the rise and fall of the soil moisture deficit (Coulthard et al., 2002) and thus influences the behaviour of the modelled flood hydrograph (Welsh et al., 2009). For example, high values of m increase soil moisture storage leading to lower flood peaks and a slower rate of recession of the hydrograph, and is therefore used to represent a well-vegetated basin (Welsh et al., 2009). Conversely, lower values of m represent more sparsely vegetated basins. In these simulations we will use values of 0.02 to represent forested basins and 0.005 for deforested. For more information on m values that have been used in previous studies, readers are directed to Beven (1997)

Equations 1 and 2 calculate a combined surface and subsurface discharge that are separated prior to routing surface runoff. This separation is carried out using a simple runoff threshold, which is a function of the hydraulic conductivity of the soil in ms^{-1} (K), the slope (S) and the grid cell size in metres (Dx) (Coulthard et al., 2002) (equation 3).

Equation 3.

$$Threshold = KS(Dx)^2$$

The volume of water above this threshold, or above a user-defined minimum value ($Q_{\min}$), is subsequently treated as surface runoff and routed using the hydraulic model.

In previous versions of CAESAR and CAESAR-Lisflood the basin response to rainfall was global – in effect a hydrograph for the basin was divided up and applied to individual cells. However, to enable spatially and temporally variable hydrology, CAESAR-Lisflood was modified so the hydrological parameters (e.g. *m* value) and precipitation rates could be input via spatially fixed pre-defined areas. For each area, a separate version of the hydrological model (equations 1-3) is run, enabling different levels of storage and runoff to be generated within each of the different areas. Here, these areas are defined with a raster index file with numbers corresponding to the areas (as described in the

179 methods) but different sub-basins or cells corresponding to different rainfall areas could be defined.
180 .All surface flow from the different hydrological areas is modelled using the same scheme – the
181 Lisflood-FP hydrodynamic flow model as developed by Bates et al., (2010) and described further in
182 Coulthard et al., (2013a). Lisflood-FP is a 2D hydrodynamic model containing a simple expression for
183 inertia. Flow is routed to a cell's four Manhattan neighbours using equation (4)

184 Equation 4.

185 $$q_{t+\Delta t} = \frac{q_t - g h_t \Delta t \frac{\partial (h_t + z)}{\partial x}}{\left(1 + g h_t \Delta t \ {}^2 q_t / {h_t}^{10/3}\right)}$$

186

187 where Δt = length of time step (s); t and $t + \Delta t$ respectively denote the present time step and the
188 next time step; q = flow per unit width (m^2/s); g = gravitational acceleration ($m\ s^{-2}$); h = flow depth
189 (m); z = bed elevation (m); and x = grid cell size (m). $\frac{\partial (h_t + z)}{\partial x}$ = water surface slope.

190 From flow depths and velocities produced by the hydraulic model, a shear stress is then determined
191 and used to drive sediment transport function to model fluvial erosion and deposition. CAESAR-
192 Lisflood provides a choice of either the Einstein (1950) or the Wilcock and Crowe (2003) method that
193 was used here. Sediment transport is then calculated for up to nine different grainsize classes that
194 may be transported as bedload or suspended load. The deposition of bed load and suspended load
195 are treated differently, with bedload is moved directly from cell to cell, whereas fall velocities and
196 sediment concentration control suspended load deposition. Importantly, the selective erosion,
197 transport and deposition of different sizes allows a spatially variable sediment size distribution to be
198 modelled. As changes in grainsize can also happen vertically as well as horizontally, a method for
199 storing sub-surface sediment data is required and this is achieved by using a system of active layers
200 with a surface active layer (the stream bed) and multiple buried layers (strata). Slope processes are
201 also simulated, with landslides occurring when a user defined slope threshold is exceeded and soil
202 creep calculated a function of slope (e.g. Coulthard et al., 2013; Van De Wiel et al., 2007).

203 2.2 Study area

204 The simulations carried out for this study are based on the River Swale in Northern England (Figure
205 1). The upper reaches of the Swale are characterized by steep valleys with the geology of
206 Carboniferous limestone and millstone grits (Bowes et al., 2003). Downstream, valleys are wider and
207 less steep, with the underlying geology Triassic mudstone and sandstones (Bowes et al., 2003). The
208 study basin covers 412 km^2, with a mean relief of 357 m, ranging between 68-712 m, and with an

209 average river gradient of 0.0064. This basin has been extensively modelled in previous studies
210 (Coulthard and Macklin, 2001; Coulthard and Van de Wiel, 2013; Coulthard et al., 2013, 2012), and a
211 pre-calibrated version of the CAESAR-Lisflood model was readily available.

212

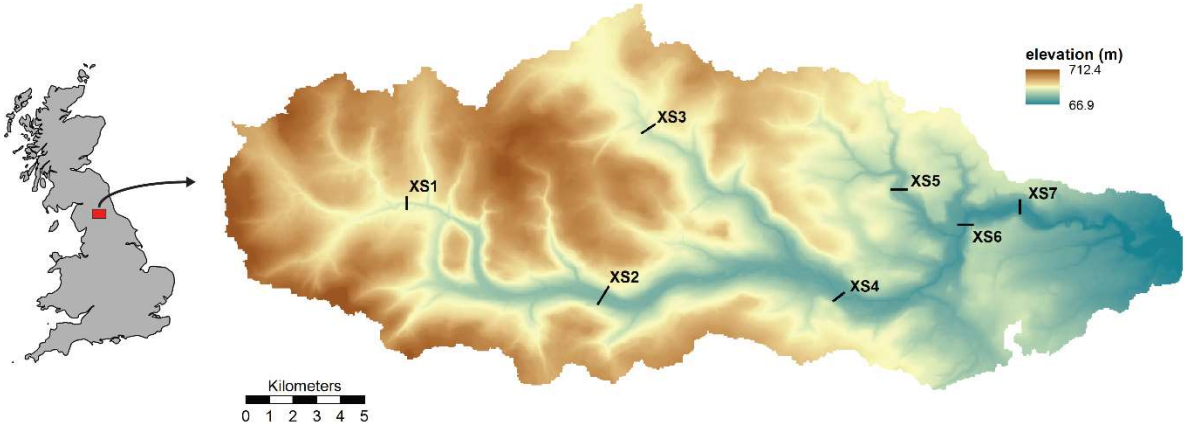

213

214 Figure 1. Elevation map of the Swale basin. Locations of cross sections used for further analysis are
215 also marked. Inset on the left shows the location of the Swale basin in the UK.

216 ## 2.3 Model configuration

217 Our numerical experiment consists of a series of model simulations in which a spatial change in land
218 cover is introduced. In each simulation the landscape is assumed to have an initial homogeneous
219 land use over the whole basin. During the simulation half of the basin is subjected to change in land
220 use, i.e. half of the basin is assigned a different m value (Figure 2A). For simplicity only two land use
221 types are considered here: grassland (m = 0.005) and forested (m = 0.02). The spatial split allows us
222 to investigate connectivity within the basin, i.e. upstream and downstream impacts of the land use
223 change can be analysed for both halves of the basin. Four change scenarios are considered (Figure
224 2A), covering all combinations of initial and final land use. Effectively, these sub-configurations
225 describe deforestation or reforestation in one half of the basin.

226

227 The transition in land use over the affected area occurs in 5 discrete phases over a 100-year period
228 between years 40 and 140 (Figure 2B). These phases correspond to a gradual expansion (in steps of
229 10% basin area) of the region affected by the land use change in each scenario, starting either at the
230 Eastern or Western edge of the basin depending on the scenario (Figure 3). The four scenarios thus
231 represent reforestation of the upper basin from the West (D1), reforestation of the lower basin from
232 the East (D2), deforestation of the lower basin from the East (D3), and deforestation of the upper
233 basin form the West (D4). After the land use change is completed, a 70-year run-out period, from
234 years 140 to 210 (Figure 2B), ensures that long-term impacts of the land use change can be

compared. Finally, as a reference, two additional simulations are run without any land use change: one with constant grassland and one with constant woodland (simulations A1 and A2, respectively). It is important to note that in this study land use change are parameterised within the CAESAR-Lisflood model to *only* alter the hydrology in the areas affected. This leads to increased or decreased surface runoff and streamflow in turn affecting erosion, but there are no changes in the strength or resistance of the surface or hillslopes to erosion. Other geomorphic effects of disturbance due to land use change (for example sediment released by tree clearance) are therefore also not considered. This also means that other feedbacks are not included, such as increasing soil depths under forest cover. Additionally, whilst our land use change scenarios are spatially progressive, they are also discrete: within each band of change we assume an instant change. This clearly would not happen in reality and while this may not be a major issue for deforestation scenarios, hydrological changes due to reforestation would occur more gradually and over longer time scales. We also have used m values to represent forested and un-forested areas that are towards the extreme of previous values used (e.g. Beven, 1997; Coulthard et al., 2000; Welsh et al., 2009). This could be viewed as provoking a larger than expected response in the basin, or alternatively as compensating for only considering the hydrological aspects of land use change and not those of soil properties of erodibility impacts. It is likely that, for example, areas experiencing deforestation hillslope surface and bank resistance to erosion would be significantly reduced – leading to even greater potential for erosion, incision and downstream aggradation. Likewise, none of the effects of re-forestation on soil properties (increased infiltration) and the effectiveness of vegetation binding sediment/soil preventing erosion are included.

For all simulations, the Swale basin was represented by a 50m digital elevation model (DEM) as illustrated in Figure 1. Precipitation inputs to the model were based on a 30 year hourly rainfall reconstruction for the Swale region created with the UKCP09 weather generator (as per Coulthard et al., 2012) that was looped to make the 210-year sequence (Figure 4). Apart from changing m values to represent different land uses (as above) all other model parameters were kept the same and these are described in Table 1. For all simulations, water and sediment yields at the basin outlet were recorded at hourly time steps, and the DEM saved every simulated year. These were used to determine sediment yields for the basin as well as to show spatial patterns of erosion and deposition. Simulation outputs are analyzed for sediment yields, patterns of erosion and deposition, volumes of erosion and deposition. First the reference scenarios A1 and A2 are analyzed. Next, simulation outputs are compared to the reference scenarios (e.g. D1 vs A1) to evaluate the impacts of the land use change. Of particular importance in these comparisons of simulation output, at least

in the context of connectivity, are erosion and deposition differences in the areas of the basin that were not subjected to a land use change. Comparisons are made at the end of the simulation, i.e. after 210 years.

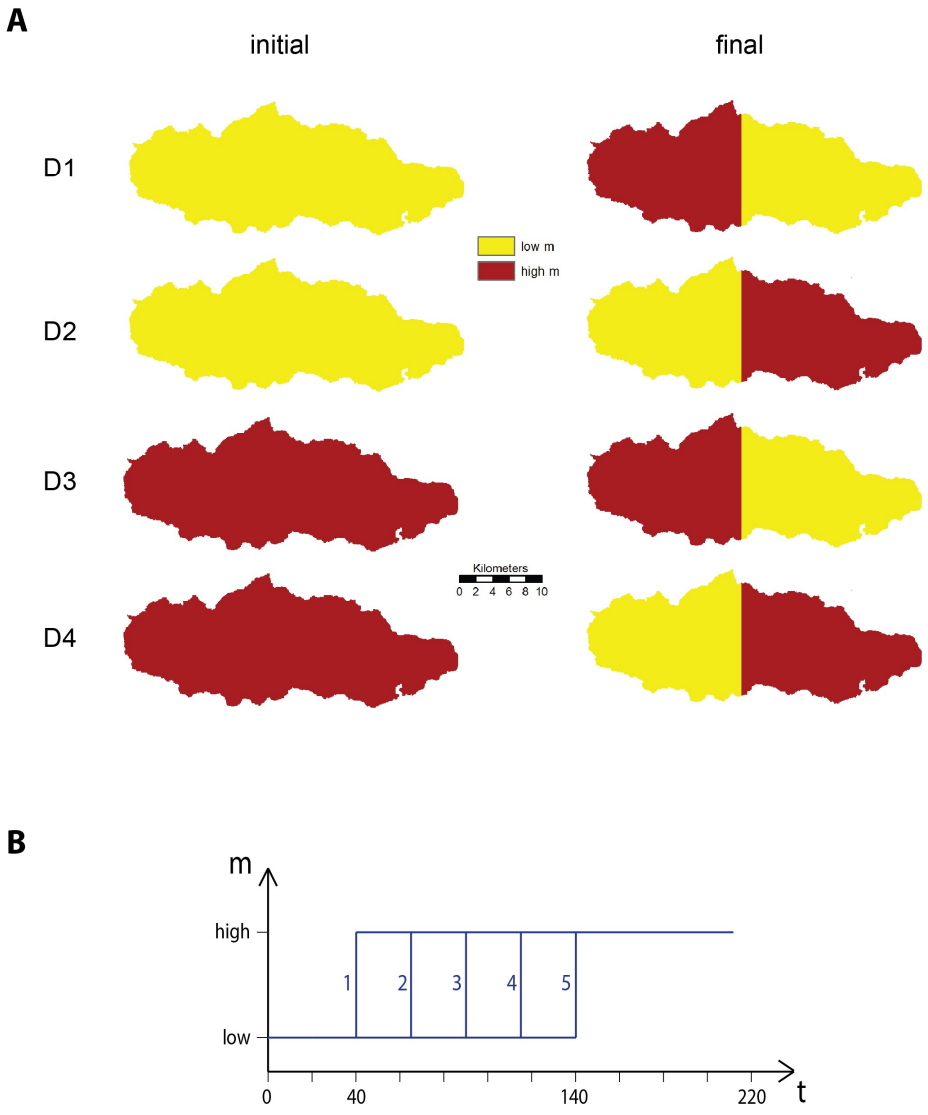

Figure 2: Overview of simulation scenarios as function of spatial and temporal variation in land use. **A)** Spatial configurations of initial and final land use. Two additional reference scenarios with constant land use (scenarios A1 and A2) are not shown here. **B)** Time series of land use m-value. Numbers (1-5) refer to five different areas of the basin, such that the land use changes occur both spatially and temporally phased (also see Figure 3).

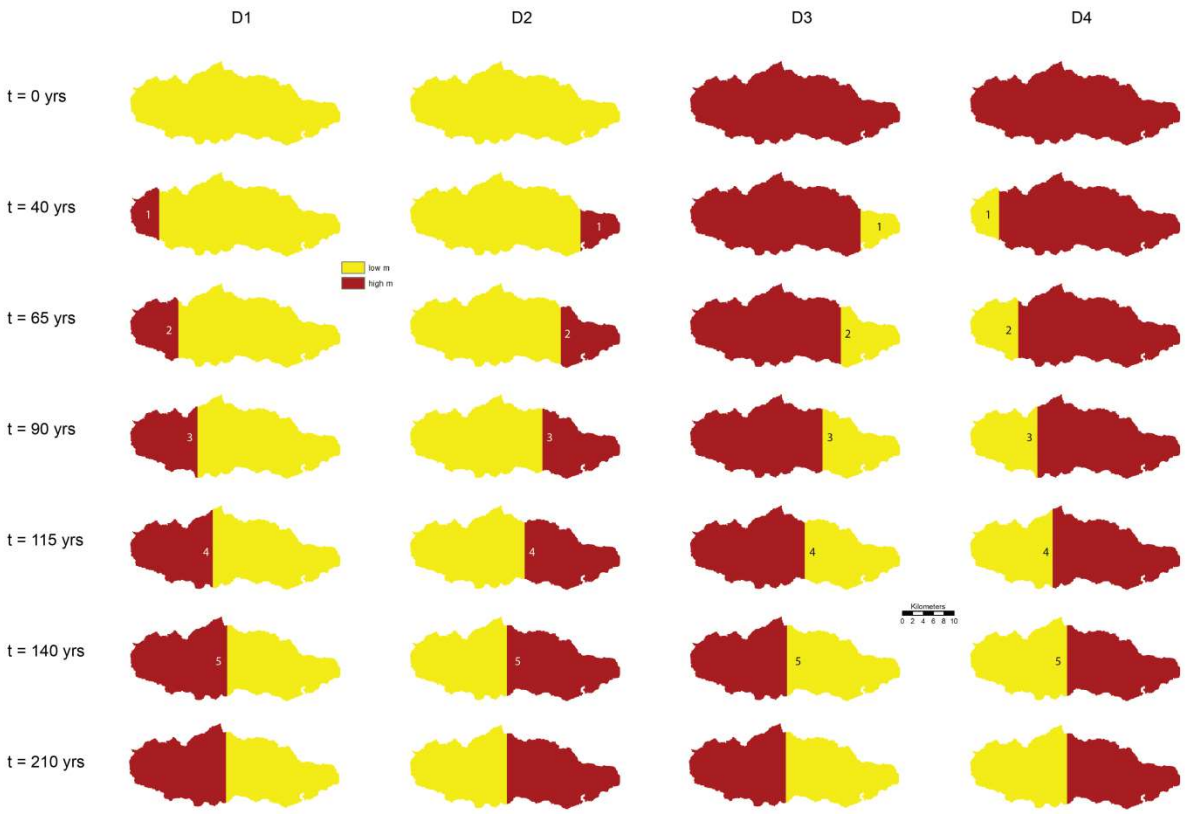

280

281 Figure 3: Snapshots of spatial configuration for the for land use change scenarios. For all scenarios
282 the land use change occurs from the extremities of the basin (East, West) towards the centre. After
283 year 140 there is no further change in land use.

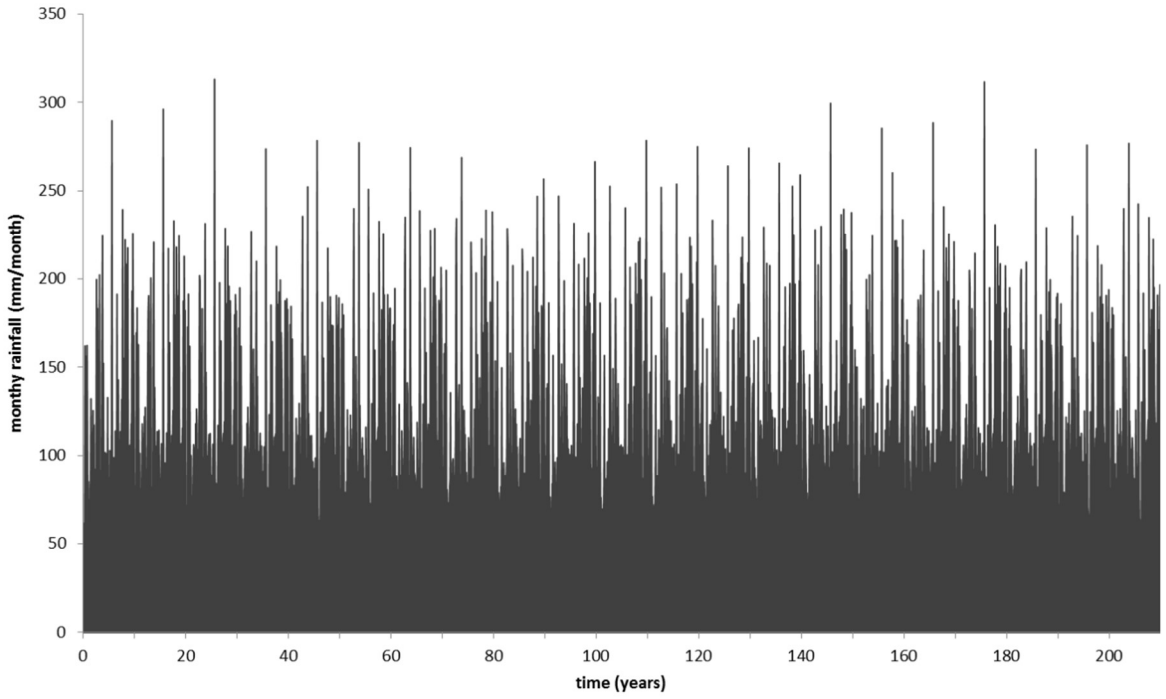

284

285 Figure 4. Pluviographs of rainfall applied in all simulations. Actual rainfall input data was provided in
286 hourly intervals rather than monthly aggregates shown here.

3. Results

For all results, the outputs from simulations A1 and A2 (completely deforested and completely forested respectively) provide control simulations against which changing land use results can be compared.

Looking first at the hydrology, Figure 5 shows how decadal summaries of the discharge drop steadily with progressive reforestation (scenarios D1 and D2) and rise similarly after deforestation (D3 and D4) before stabilising after basin land use changes end at 130 years. For D2 and D3 where the Eastern side of the basin was re/de-forested the changes are slightly greater than in D1 and D4. Interestingly, both scenarios converge to the same point, indicating that there is no hydraulic legacy of the initial land use.

Decadal sediment yield totals from the basin outlet clearly shows how changes in basin land use have an impact upon the sediment delivery (Figure 6) that broadly, though not completely mirror the response of the hydrology. Scenarios D1 and D2 (reforestation of top and bottom) both show a marked reduction in sediment yield from the A1 deforested scenario, with the reduction occurs progressively with the addition of more forested areas. In contrast to the hydrology, reforestation of the Western (upper) half of the basin (D1) leads to a greater reduction in sediment yield than reforestation of the Eastern (lower) half – suggesting the steeper gradient headwaters are important for generating basin wide sediment loads. For deforestation scenarios, D3 and D4 generate significant increases in sediment yield with a greater than 300% increase from the A2 baseline. As per the reforestation scenarios the changes occur progressively as more of the basin is deforested. Changes in sediment yield for all four of the change scenarios (D1-D4) occur rapidly with no apparent lag. Furthermore, D1-D4 all converge towards similar decadal sediment totals as the simulations close (Figure 6). The general decline in sediment yields compared to the hydrology is caused by the gradual exhaustion of readily transportable sediment supply.

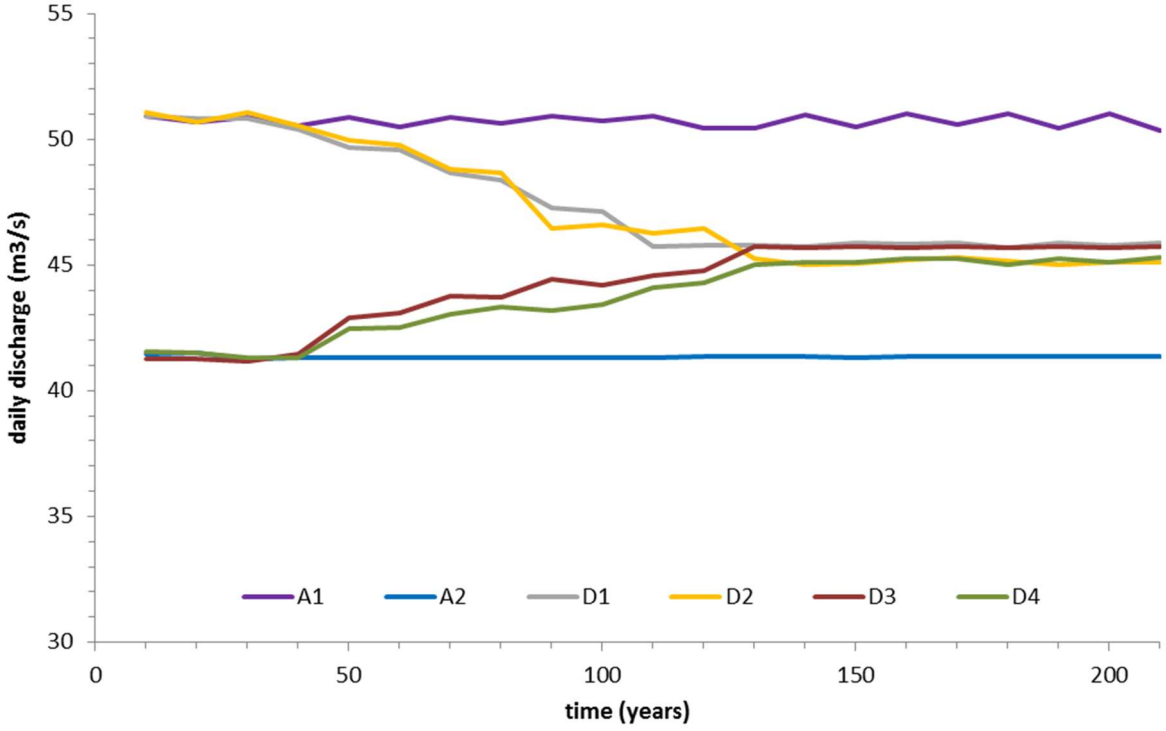

314

315 Figure 5: Decadal discharge regime from simulations A1, A2,and D1-D4. The graphs show the decadal
316 95th percentile of average daily discharge values. Note non-zero origin on Y-axis.

317

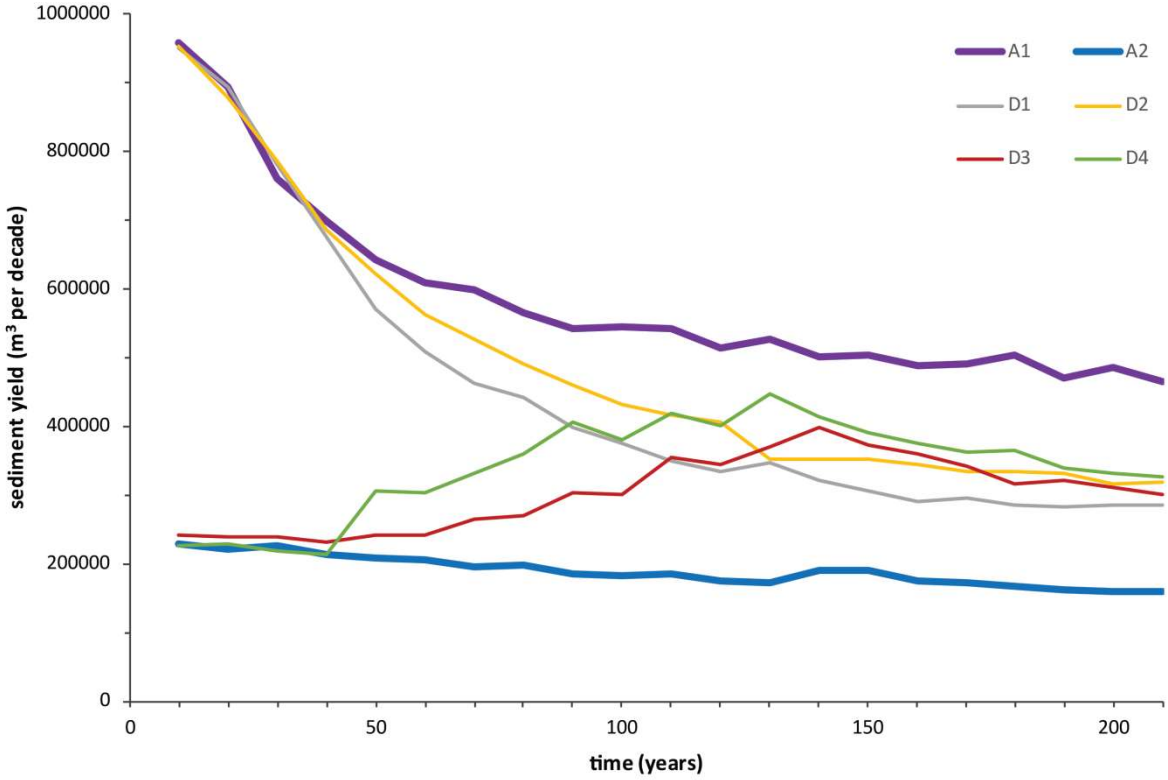

318

319 Figure 6. Decadal sediment yields from simulations A1, A2 and D1-D4.

320

321

Table 2. Descriptive statistics of erosion and deposition in scenarios A1-A2 and D1-D4, after 210 years.

	A1		A2		D1		D2		D3		D4	
	West	East	West	East	West	East	West	East	West	East	West	East
erosion (> 1cm)												
total (km^3)	0.0104	0.0131	0.0037	0.0042	0.0065	0.0115	0.0102	0.0102	0.0038	0.0082	0.0085	0.0057
area (km^2)	16.97	18.02	9.97	11.33	15.06	17.97	17.00	16.69	11.52	16.83	15.85	13.68
maximum (m)	28.276	23.756	16.501	24.777	18.988	24.170	27.749	23.677	16.266	24.525	25.273	24.681
average (m)	0.612	0.729	0.372	0.373	0.429	0.641	0.602	0.614	0.330	0.487	0.534	0.418
std dev (m)	1.625	1.807	0.693	0.773	1.038	1.563	1.608	1.497	0.660	1.158	1.498	0.969
deposition (>1 cm)												
total (km^3)	0.0051	0.0062	0.0022	0.0019	0.0035	0.0051	0.0051	0.0053	0.0023	0.0035	0.0046	0.0026
area (km^2)	8.29	8.39	6.51	6.41	8.23	8.29	8.27	8.04	7.31	8.37	8.42	6.73
maximum (m)	5.519	7.138	5.538	3.720	6.294	7.073	5.582	7.388	5.606	6.620	5.919	5.386
average (m)	0.616	0.744	0.333	0.291	0.430	0.620	0.614	0.658	0.309	0.418	0.541	0.387
std dev (m)	0.869	1.004	0.459	0.373	0.626	0.814	0.858	0.934	0.441	0.574	0.774	0.590

322

323 Table 2 divides the erosion and deposition totals between the Western and Eastern sides, allowing
324 us to see how the changes impact on the different sides of the basin. In reforestation scenario D1,
325 there is a 40% reduction in erosion for the Western upper part of D1 where reforestation occurred,
326 relative to reference scenario A1. In the Eastern lower part, without land use change, there is a
327 smaller 15% reduction in erosion. For scenario D2 erosion totals for the upper unaffected part are
328 very similar to reference scenario A1, with only a 19% reduction in erosion for the reforested lower
329 part. In both reforestation scenarios, the decrease in erosion is largely due to a reduction in average
330 erosion at each point, rather than a reduction in the area of erosion. In deforestation scenario D3,
331 there is little change for the upper unaffected parts relative to reference scenario A2, but a 100%
332 increase in erosion for the lower Eastern side where the deforestation occurred. With D4, the
333 deforested Western side gives a 130% increase in erosion relative to A2 and the unchanged lower
334 Eastern side a 35% increase. In both parts there not only an increase in average erosion at each
335 point, but also in area affected by the erosion (60% for the Western upper part, and 20% for the
336 Eastern lower part). Each scenario has less deposition than erosion in both halves of the basin, but
337 overall responses in deposition are similar to responses in erosion.

338

339 The spatial patterns of erosion and deposition (Figures 7 – 9) show the elevation changes caused by
340 erosion and deposition at the end of the 210 year simulations for the baseline scenarios A1 and A2,
341 and for land use change scenarios D1 to D4. In addition, seven cross sections corresponding to the
342 locations marked on Figure 1 are presented in Figures 10-13. Comparing A1 and A2, there is clearly
343 more erosion in the headwaters and tributaries of the deforested A1 baseline (Figure 7). Whilst this
344 is also reflected in the basin sediment yields (Figure 6), the spatial patterns also illustrate there is

345 extensive deposition of the eroded material on the valley floors (Figure 7E, inset 2 and 3), with the
346 channel incising to one side of the valley, creating a river terrace. This can also be seen in the cross
347 section data (Figures 10-13), notably in the incision of headwaters and tributaries in XS1 and XS3, as
348 well as for the terraces shown in XS4 and XS7.

349 Looking at the spatial patterns of erosion and deposition for the reforestation (D1 and D2) and
350 deforestation (D3 and D4) scenarios in Figure 8, the patterns largely reflect those indicated in Table
351 2 with the greatest changes in the areas disturbed. There is clearly less incision in the Western
352 headwaters of D1 when compared to D2, while similar patterns are shown in the Eastern section,
353 though here with less incision in D2 reflecting the reforestation of the Eastern side. There are some
354 notable differences, however, when more closely examined. For example, the Eastern side of the
355 major Northern tributary in D1 is less incised – despite being in a deforested area as the headwaters
356 of this tributary are in the Western side lie in a region that becomes reforested, thus reducing
357 stream powers and erosion downstream. For the deforestation simulations (D3 and D4) patterns are
358 more straightforward, with increased erosion in steeper headwaters linked to increased deposition
359 in the lower gradient valley floors when the Western and Eastern sides, respectively, are deforested.

360 These effects are even more clearly shown in Figures 9A, D, G, J where the differences in elevation at
361 the end of the 210 years between the scenario runs (D1-D4) and their respective baselines (A1 and
362 A2) are plotted. Here, the upstream areas of the Western side of D1 (Figure 9A inset 1) show clearly
363 that the reforestation of that area in D1 leads to far less (30% less average erosion; Table 2) of
364 incision as well as considerably less deposition in the valley floors (Figure 9A inset 3, 45% less
365 average deposition; Table 2). The lower Eastern part of the basin in D1 has experienced the same
366 hydrology as A1 so all changes in this part of D1 are due to the upstream changes. This unexpectedly
367 includes small increases in incision in the lowest northern tributary (Figure 9A). Also of interest are
368 changes in the Western side of D2 (Figure 9D), where the hydrology and flood magnitudes have
369 remained the same in both A2 and D2, yet there is slightly more incision in D2.

370

371 For deforestation scenarios D3 and D4, the spatial patterns again largely reflect where the
372 deforestation has occurred (Figures 9G and 9K). More headwater incision and valley floor deposition
373 is found in the Eastern side of D3 and the Western side of D4 (Figure 9K, inset 1), i.e. the sides
374 deforested. As with the un-forested scenarios (Figures 9A and 9D), there are also differences – in
375 some cases greater than 1m – in areas where the land use was unchanged, for example in the
376 Western side of D3 (Figure 9G) and the Northern tributaries of the Eastern side of D4 (Figure 9K).
377 Notably, this can happen both upstream and downstream of where the deforestation occurred.

In summary – disturbance (reforestation or deforestation) has the greater impact on the area where it occurs, significantly changing erosion and deposition patterns. Additionally, there are impacts generated from both disturbances downstream and lesser changes upstream.

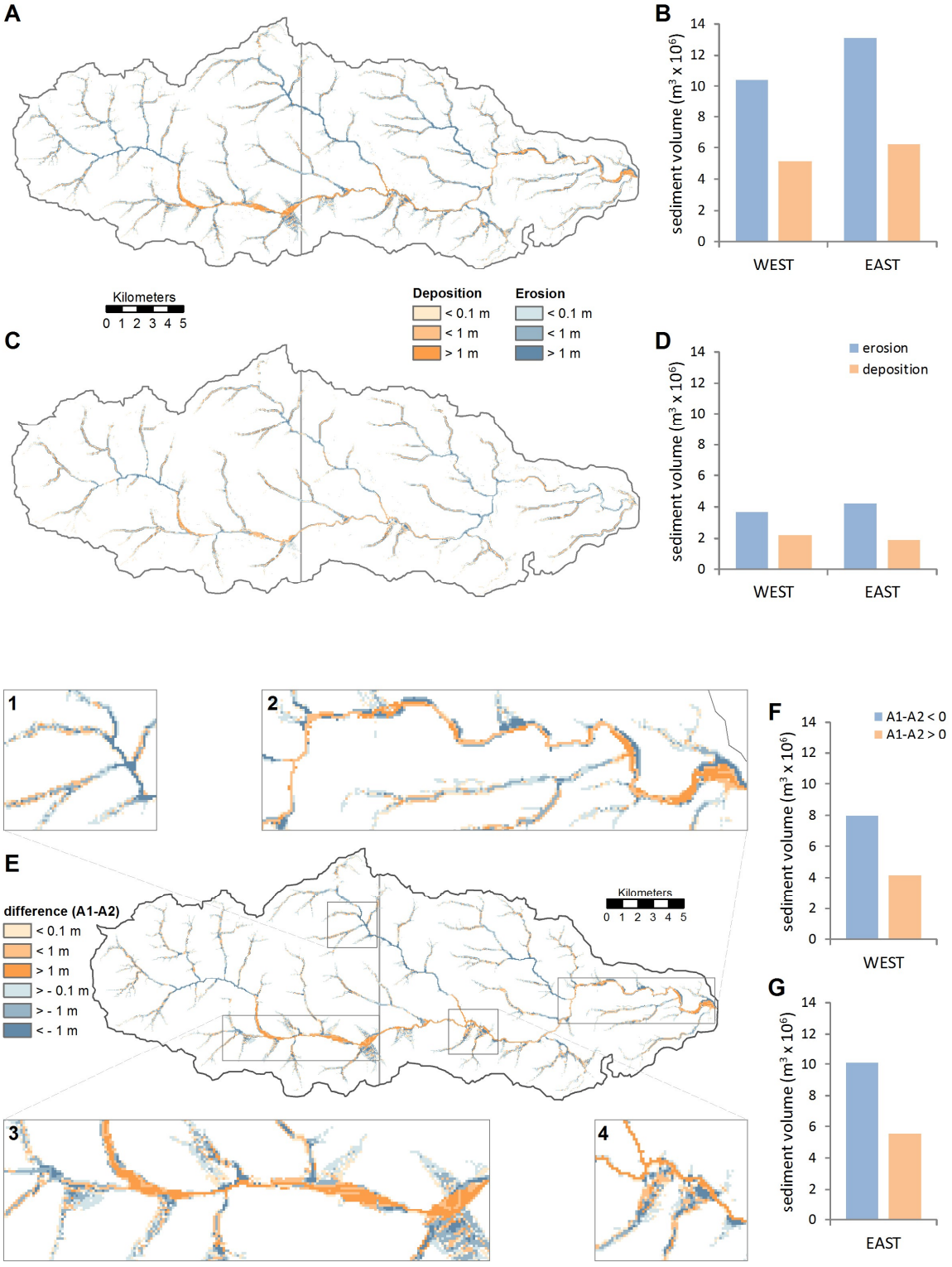

383

384 Figure 7. Erosion and deposition at year 210 in the reference scenarios A1 (A) and A2 (C), and the
385 difference between the two (E). In the bottom map the colours represent the status of A1 relative to

A2, i.e. where A1 is lower than A2 (blue) or where A1 is higher than A2 (orange). Bar charts B, F, H and G show the volumes of sediment eroded and deposited as also shown in Table 2.

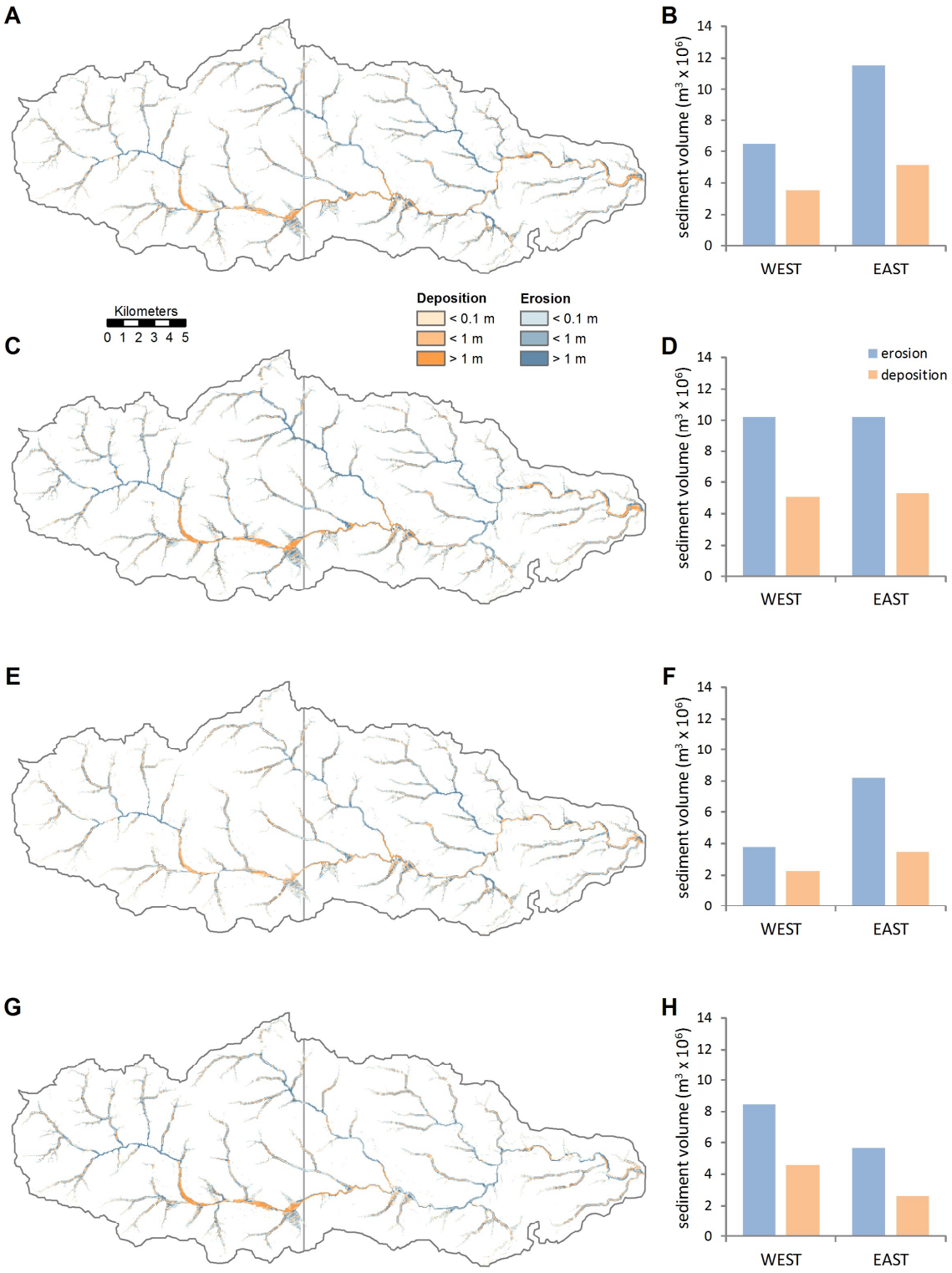

389 Figure 8. Patterns of erosion and deposition at year 210 in scenarios D1-D4 compared to the initial
390 DEM surface.

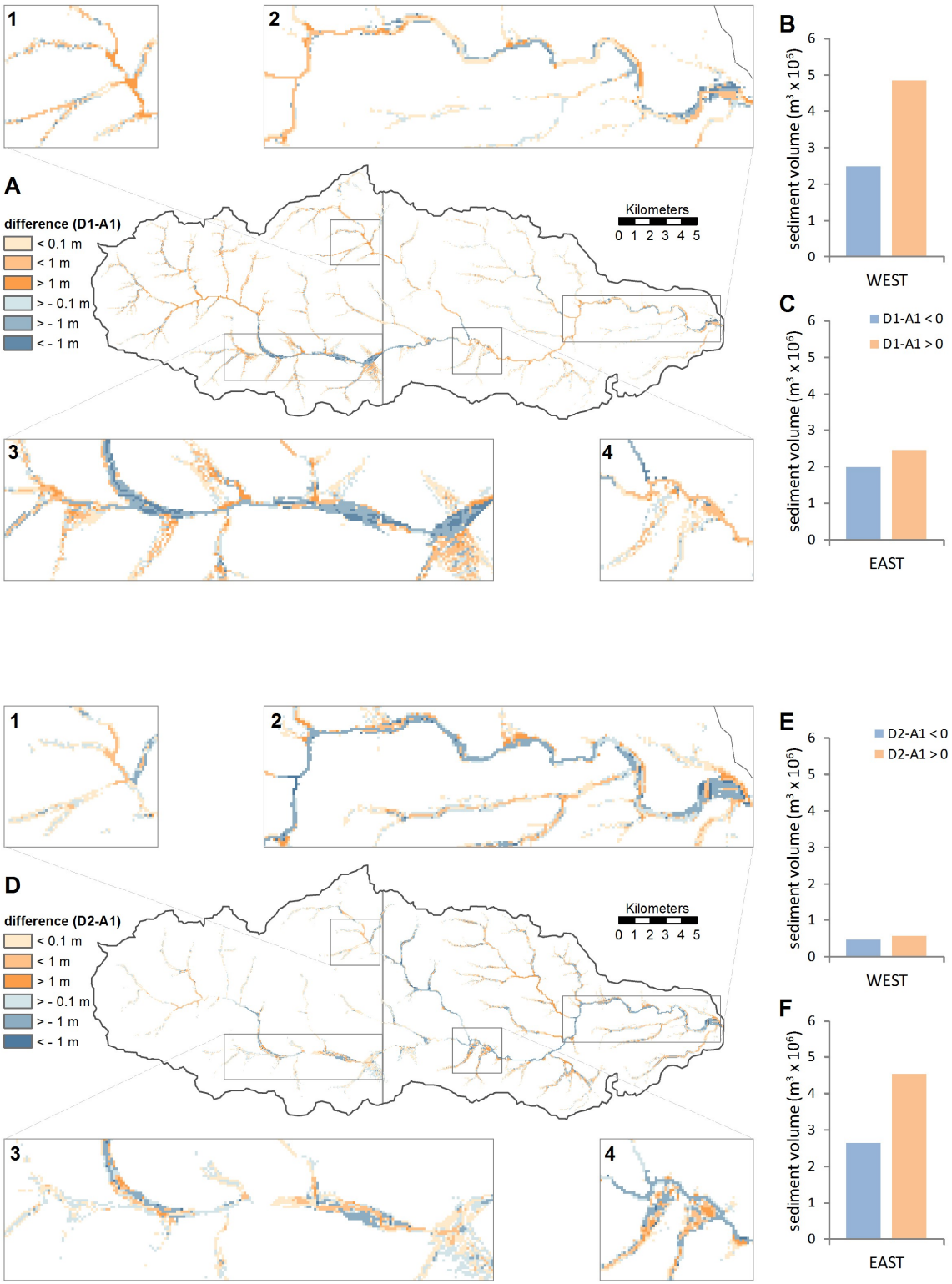

391

Figure 9A. Difference in erosion and deposition at year 210 for scenarios D1-D4, relative to reference scenario with the same initial land use (A1 or A2). Colours indicate where scenarios are higher or lower in elevation than the reference scenario.

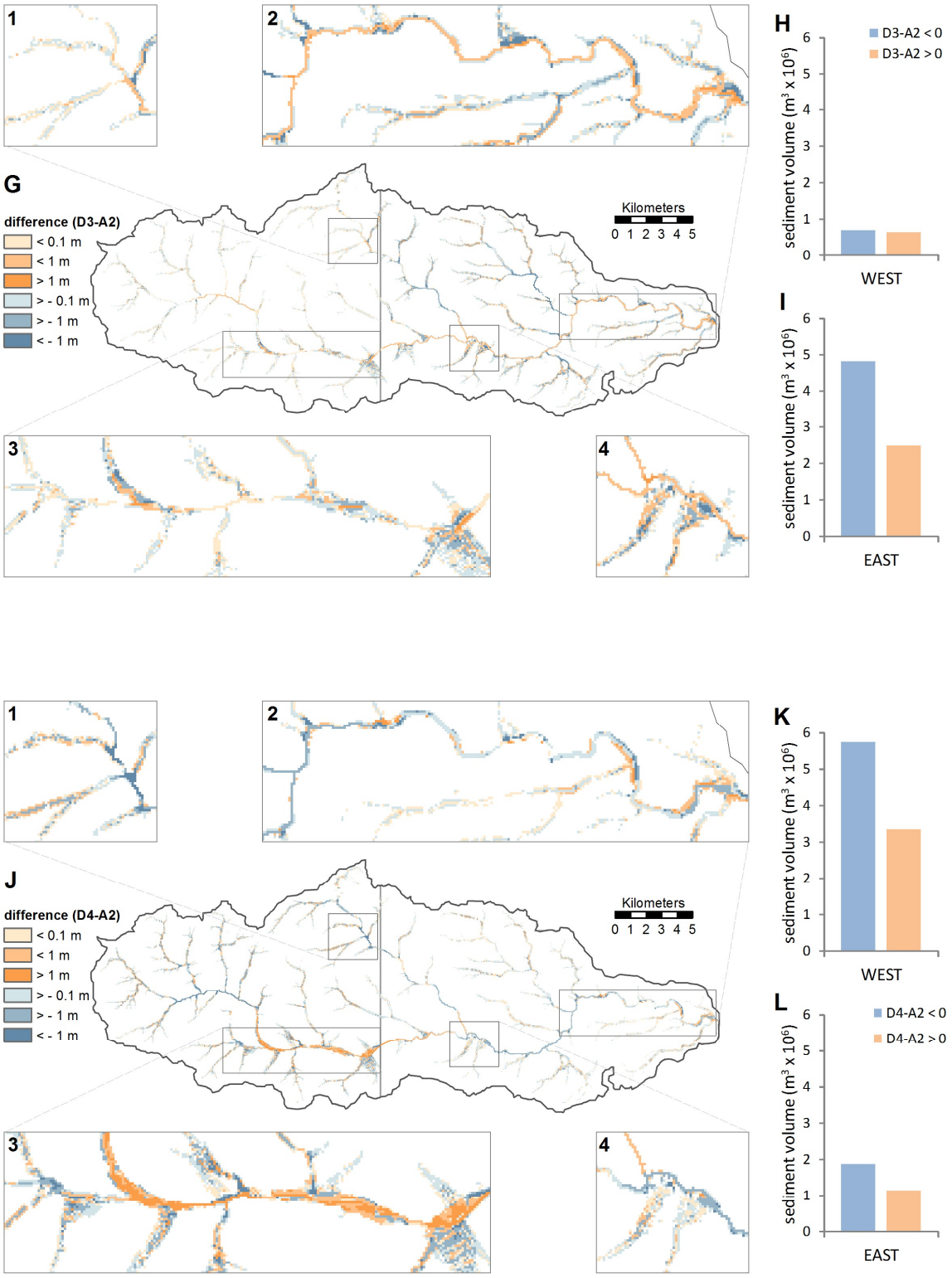

396 Figure 9B. Difference in erosion and deposition at year 210 for scenarios D1-D4, relative to reference
397 scenario with the same initial land use (A1 or A2). Colours indicate where scenarios are higher or
398 lower in elevation than the reference scenario.

399

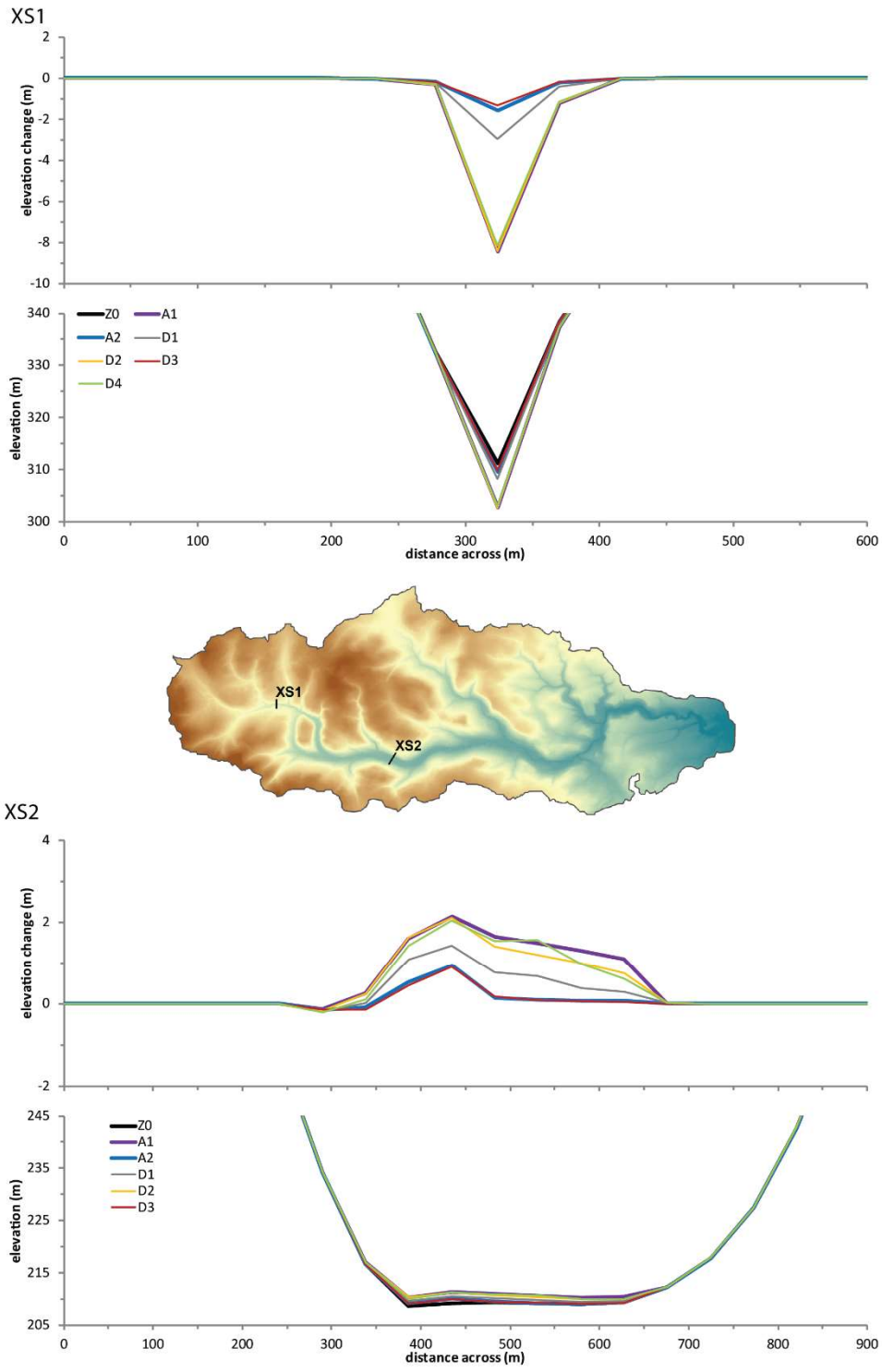

400

401 Figure 10. Cross sections 1 and 2.

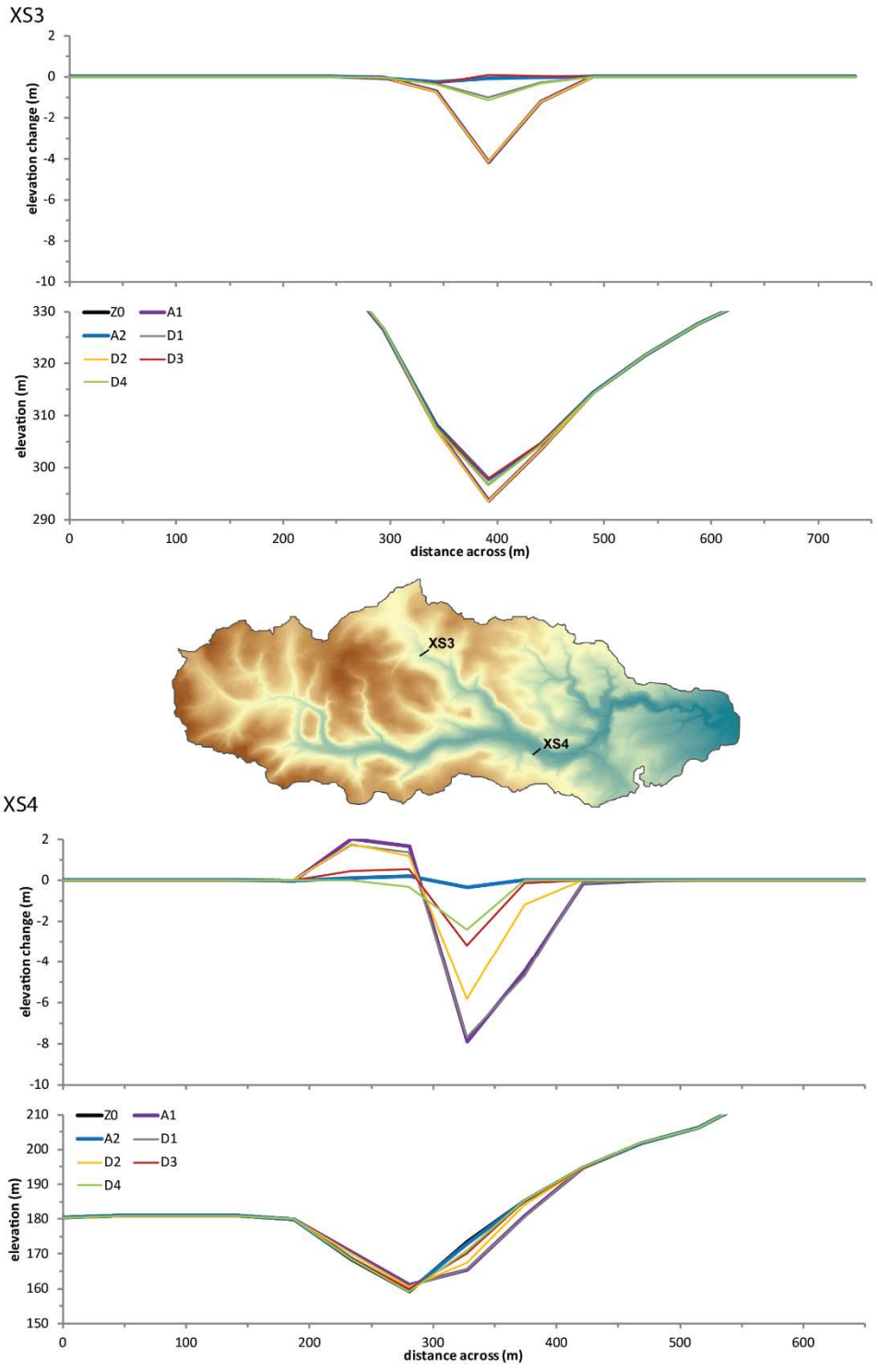

402

403 Figure 11. Cross sections 3 and 4.

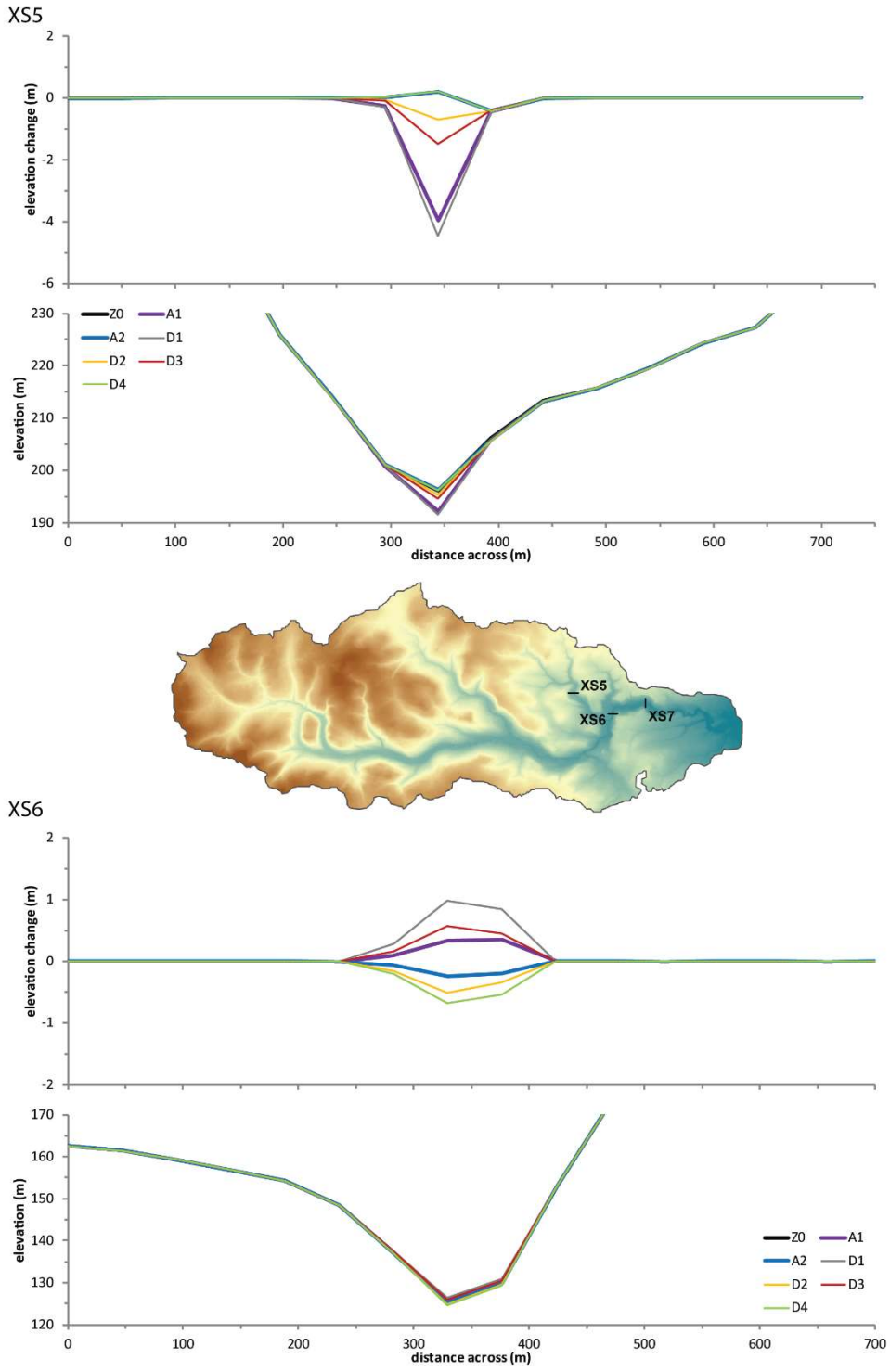

404

405 Figure 12. Cross sections 5 and 6.

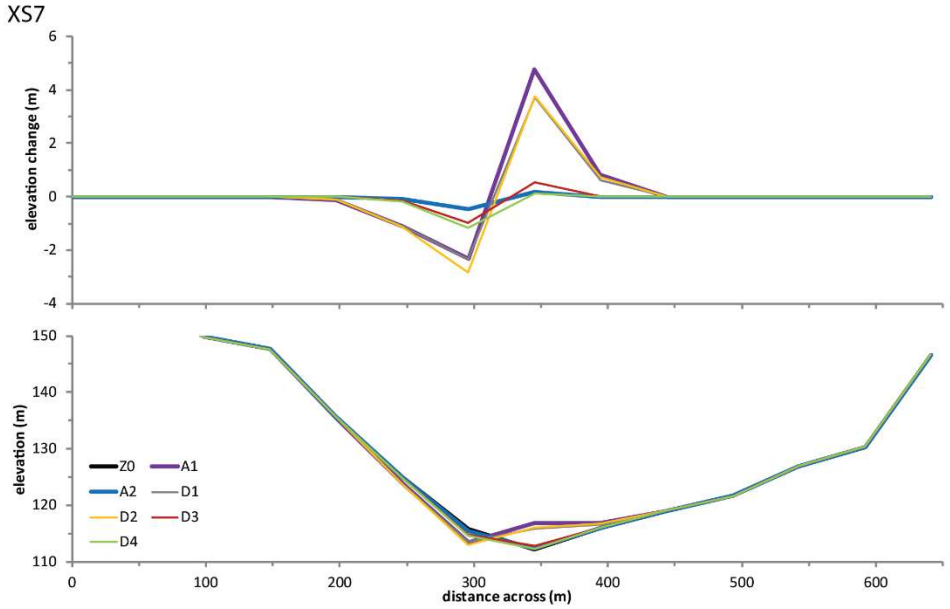

406

407 Figure 13. Cross section 7.

408

409 ## 4. Discussion

410 Changes in land use in both upper and lower parts of the basin, both reforestation and deforestation
411 lead to significant changes in the hydrology and the lumped basin sediment yields (Figure 5 and 6,
412 Tables 2 and 3) suggesting a high level of sediment connectivity driven by the hydrology. Changes in
413 land use are reflected rapidly in sediment totals, with increases or decreases in sediment delivery
414 responding linearly with the increase in de or reforestation. There are, however, relative differences
415 between the impact of land use change in the Western (upper) and Eastern (lower) sides, with
416 greater reductions in sediment delivery from reforestation in the West than lower East sides, and
417 greater increases associated with deforestation in the West than East. This could be due to the
418 Western (upper side) being largely more upland, with steeper gradients and streams more likely to
419 respond vertically to changes in the hydrology. Though previous modelling work (Coulthard and Van
420 de Wiel, 2013) using the same model showed that lumped basin sediment outputs were more
421 sensitive to changes in climate (hydrology) than local gradient changes due to tectonics. Therefore,
422 for D1 and D4 with Western (upstream) changes in land use, changes in basin sediment outputs are
423 less due to changes in sediment delivery from these upstream areas, but more influenced by
424 increases (or decreases) in flood magnitudes and erosion patterns downstream. Interestingly, all
425 four scenario runs (D1-D4) trend towards the same lumped decadal sediment yield at the end of the
426 210 year simulations where similar proportions of the basin are forested and deforested. This

indicates that for the River Swale, the basin settles to a new stable state within 50 or so years and that for lumped sediment outputs the precise location of forested and deforested areas is not crucial. For management downstream of this basin, these model results indicate that reforestation and deforestation make significant changes in the size of floods and the volumes of sediment leaving the basin. This implies that such wholesale changes in land use (here up to 50% by area) can be viable methods for reducing flood risk and sedimentation issues though it must be remembered that our land use changes are not calibrated.

However, the spatial patterns of erosion and deposition (Figures 7-9) show the lumped sediment yield figures mask subtle and nuanced variations in where erosion and deposition are happening within the basin. There are major local variations in patterns of erosion and deposition, with morphological changes in the channel and valley floor strongly linked to where the changes in land use are. Broadly, in deforested areas there is an increase in headwater incision and valley floor deposition due to increased and flashier discharges (as identified by Harvey, 1996), whereas in reforested regions there is less incision and valley floor deposition. This is evidenced by the incision shown in the cross sections (Figures 10-13) as well as the river terraces formed at XS 4 and 7. Morphological changes due to land use change are also expressed horizontally as well as vertically. In deforested areas increased erosion is partly due to the expansion of drainage network (reflected in the eroded area; Table 2), as well as an increase in the average erosion amount (considering the mean of all cells where erosion occurs; Table 2).

Of great interest for basin connectivity are the erosion, deposition and morphological changes outside of the areas affected by land use change. These occur downstream, for example in D1 (Figures 8A, 9A, B, C). Compared to baseline scenario A1, upstream reforestation in D1 results in less erosion in the upland headwaters (indicated as orange in Figure 9A) and consequently less deposition in the central upland valley (indicated as blue). The downstream Eastern part shows a complex interplay between localised erosion and deposition (orange and blue) in the Eastern river valleys which is different from the A1 scenario (mix of blues and oranges). These downstream differences can be attributed to altered hydrological control from the reforested headwaters, and to the associated reduced upstream sediment delivery (Figure 9B) which would affect local erosion and deposition potential in the downstream areas (Figure 9A, 9C). A similar downstream effect can be observed when comparing scenario D4 (upstream deforestation) to baseline scenario A2 (no deforestation), where the increased flow from the deforested uplands increases erosion potential in the downstream area, but also delivers additional sediment (Figure 9K) resulting in shifted erosion and deposition patterns in the downstream part that was not directly affected by the land use change (Figure 9J, 9L). Such downstream impacts are clear examples of land use connectivity

affecting both hydrology and sediment, although the downstream transmission of connectivity impacts is both logical and expected since it occurs in the direction of flow and gravity.

More unexpected are the transmission of changes in erosion and deposition *upstream* from where the changes happen. In scenarios D2 and D3 there are several examples of where changes in erosion and deposition have occurred upstream of where land use changes have occurred in the downstream, Eastern side. These changes occur under both downstream deforestation and reforestation, are mainly found in the valley floor and extending a considerable distance towards the head of the basin (Figures 9D, 9G). This indicates a *reverse connectivity* in the landscape, whereby changes in the base level of the central valley floor many kilometres downstream are altering patterns of erosion and deposition upstream. Yet, though widespread through the valley network, the reverse connectivity changes are subtle in magnitude. The impact on net sediment yield in the upstream areas is low, as sediment volume differences with the baseline scenarios are about equal for higher (orange) and lower (blue) elevations (Figures 9E, 9H). This *reverse connectivity* is also evident in the other smaller Northern tributary that is affected by downstream changes independent of the main valley. In Figure 9A, the Eastern side of D1 and D4 (Figure 9J), where again base level changes in the main channel and valley floor are transmitted up the tributaries (For example, the difference between A1 and D1 in XS5 - Figure 12).

Overall, the downstream connectivity in scenarios D1 and D4 is stronger (Figures 9C, 9L) than the *reverse connectivity* in scenarios D2 and D3 (Figures 9E, 9H). Nonetheless, a reverse connectivity is clearly demonstrated. Such behaviour is maybe expected where there are significant changes in base level due to tectonic uplift or sea level changes, for example leading to the upstream migration of nick points. However, here such a response was unexpected and this may be the first time such upstream geomorphic change has been attributed to downstream land use changes. Sediment outputs and geomorphic response to changes is often non linear in both natural and simulated drainage basins (e.g. Coulthard and Van De Wiel, 2007; Schumm, 1973; Temme et al., 2015) and may exhibit a sensitivity to initial conditions and drivers. Therefore, it is possible that any small downstream changes could have an impact upstream. However, the changes we have recorded due to downstream changes, whilst not as great as those due to upstream changes are up to 2m in magnitude. Notwithstanding this, these results clearly indicates that there is an upstream sensitivity within these simulations to downstream changes. Referring back to the connectivity literature, within the erosion and deposition maps of our basin simulations there is widespread evidence of Fryirs et al., (2007)'s sediment buffers, barriers and blankets. These can be found in the large deposits of sediment left in the valley floor by upland incision, downstream areas of alluviation and

aggradation as well as base level effects where deposition leads to the backing up of sediment delivered from upstream tributaries.

Considering our findings in the context of Holocene alluviation, the model results clearly show that de- and re-forestation can have a major change on basin wide sediment delivery as well as on local erosion and alluviation. Indeed, our simulations readily produced river terraces – backing up previous research suggesting these could be caused by changes in land use (e.g. Brown and Barber, 1985). Of interest to those trying to reconstruct past land use changes from alluvial geomorphology are that areas of erosion and deposition were closely linked (spatially) to where the land use changes occurred. Whilst there was some downstream alluviation in D4 (Western side deforested), the greatest amounts were to be found in the areas deforested (Figures 9K, 9L). Our results (especially for upland deforestation, D4) chime with several field studies mentioned in the introduction as well as for the Bowland Fells (Harvey and Renwick, 1987) and the Hodder basin in NW England. Here, upland forest clearance and the expansion of moorland and pasture led to headwater erosion and downstream aggradation. Additionally, there is the added complication of base level changes leading to smaller patterns of erosion and alluviation in areas unaffected by land use changes, even upstream. If trying to reconstruct land use changes from downstream areas, our findings indicate that deforestation in the headwaters has a slightly greater impact than deforestation lower down (D4 vs D3) but as the decadal sediment totals trend towards each other (Figure 6) over longer time scales the precise location of deforestation matters less. Put simply, areas of deforestation have a significant local effect, but role of the location of deforestation is buffered when considering the basin totals.

It is important to consider, that the upstream and downstream connectivity impacts shown in these simulations are driven solely by the hydrology, with deforestation/reforestation changing the amount of water added at different places within the basin. This in turn will alter channel flows, velocities, shear stresses and thus erosion. Within the model parameterisation no changes are made to the ability of sediment movement to move, grainsize nor sediment availability, or to any hydraulic or roughness parameters.

One tool that has previously been used to assess sediment connectivity over a basin is the Sediment Delivery ratio or SDR (Walling, 1983). This can be simply defined as the net erosion divided by the total erosion in a basin (Brierley et al., 2006). For our simulations, compared against the baselines there are very small decreases in SDR's due to reforestation (D1, D2 vs A1) and similarly small increases in SDR's linked to deforestation (D3, D4 vs A2) (Table 3). These changes are in line with what might be expected, but are slight in comparison to the level of basin disturbance and this leads

us to question whether the SDR is an appropriate tool for measuring connectivity using basin wide figures. Using SDR over shorter, for example, reach based examples may be more appropriate.

Table 3. Sediment yield and delivery ratios for scenarios A1-A2 and D1-D4, after 210 years.

	A1	A2	D1	D2	D3	D4
total erosion (km^3)	0.0238	0.0082	0.0183	0.0208	0.0123	0.0145
total deposition (km^3)	0.0115	0.0042	0.0089	0.0106	0.0060	0.0074
sediment yield (km^3)	0.0123	0.0040	0.0094	0.0103	0.0064	0.0071
sediment delivery ratio (%)	51.6	48.3	51.5	49.3	51.7	49.3

5. Conclusions

Our simulations show that land use change (deforestation or reforestation) not only impacts the geomorphology of the areas affected by the land use change, but also other parts of the landscape. This evidences a sediment connectivity in the simulated basin which influences geomorphological processes across the basin. This connectivity, driven by land use changes, is locally very high, with significant morphological changes close to where de- or re-forestation occurs. However, the connectivity is still apparent in the basin scale sediment yields, as deforestation of half the basin can increase decadal sediment yields by over 100%, whereas reforestation of half the basin can lead to 40% decreases. Changes in land use are quickly reflected in basin sediment yields and increases or decreases in sediment output are commensurate with the size of the areas changed. Alluviation of valley floors due to deforestation occurs not only close to the site of change but can also occur some distance downstream. Also, and unexpectedly, erosion and deposition can be triggered *upstream* from changes, due to alterations in the valley floor base level due to incision and alluviation. Importantly, this *reverse connectivity* shows how changes in the basin are not only passed in a downstream direction.

Acknowledgements

The authors would like to especially thank the two anonymous reviewers for highly constructive observations and comments on our findings, that have helped place them in a far better context. The research was partly funded by NERC grant number NE/K008668/1 “Susceptibility of catchments to INTense RAinfall and flooding (Project SINATRA)”. The CAESAR-Lisflood model is freely available via http://www.coulthard.org.uk

Bibliography

Baartman, J.E.M., Masselink, R., Keesstra, S.D., Temme, A.J. a M., 2013. Linking landscape morphological complexity and sediment connectivity. Earth Surf. Process. Landforms 38, 1457–1471. doi:10.1002/esp.3434

Ballantyne, C.K., 1991. Late Holocene erosion in upland Britain: climatic deterioration or human influence? The Holocene 1, 81–85. doi:10.1177/095968369100100111

Bates, P.D., Horritt, M.S., Fewtrell, T.J., 2010. A simple inertial formulation of the shallow water equations for efficient two-dimensional flood inundation modelling. J. Hydrol. 387, 33–45. doi:10.1016/j.jhydrol.2010.03.027

Beven, K.J., 1997. TOPMODEL: A critique. Hydrol. Process. 11, 1069–1085. doi:10.1002/(SICI)1099-1085(199707)11:9<1069::AID-HYP545>3.0.CO;2-O

Beven, K.J., Kirkby, M.J., 1979. A physically based, variable contributing area model of basin hydrology / Un modèle à base physique de zone d'appel variable de l'hydrologie du bassin versant. Hydrol. Sci. Bull. 24, 43–69. doi:10.1080/02626667909491834

Bork, H.R., Lang, A., 2003. Quantification of past soil erosion and land use/land cover changes in Germany. Long term hillslope Fluv. Syst. Model., Lecture Notes in Earth Sciences 101, 231–239. doi:10.1007/3-540-36606-7

Bowes, M.J., House, W. a., Hodgkinson, R. a., 2003. Phosphorus dynamics along a river continuum. Sci. Total Environ. 313, 199–212. doi:10.1016/S0048-9697(03)00260-2

Bracken, L.J., Croke, J., 2007. The concept of hydrological connectivity and its contribution to understanding runoff-dominated geomorphic systems. Hydrol. Process. 21, 1749–1763. doi:10.1002/hyp.6313

Brierley, G., Fryirs, K., Jain, V., 2006. Landscape connectivity: the geographic basis of geomorphic applications. Area 382, 165–174.

Brown, A.G., 2002. Floodplain landscapes and archaeology: fluvial events and human agency. J. Wetl. Archaeol. 2, 89–104.

Brown, A.G., Barber, K.E., 1985. Late Holocene paleoecology and sedimentary history of a small lowland catchment in central England. Quat. Res. 24, 87–102. doi:10.1016/0033-5894(85)90085-7

Burrin, P.J., 1985. Holocene alluviation in Southeast England and some implications for

582 palaeohydrological studies. Earth Surf. Process. Landforms 10, 257–271.
583 doi:10.1002/esp.3290100308

584 Castelltort, S., Van Den Driessche, J., 2003. How plausible are high-frequency sediment supply-driven
585 cycles in the stratigraphic record? Sediment. Geol. 157, 3–13. doi:10.1016/S0037-
586 0738(03)00066-6

587 Coulthard, T.J., Kirkby, M.J., Macklin, M.G., 2000. Modelling geomorphic response to environmental
588 change in an upland catchment. Hydrol. Process. 14, 2031–2045. doi:10.1002/1099-
589 1085(20000815/30)14:11/12<2031::AID-HYP53>3.0.CO;2-G

590 Coulthard, T.J., Lewin, J., Macklin, M.G., 2005. Modelling differential catchment response to
591 environmental change. Geomorphology 69, 222–241. doi:10.1016/j.geomorph.2005.01.008

592 Coulthard, T.J., Macklin, M.G., 2001. How sensitive are river systems to climate and land-use
593 changes? A model-based evaluation. J. Quat. Sci. 16, 347–351. doi:10.1002/jqs.604

594 Coulthard, T.J., Macklin, M.G., Kirkby, M.J., 2002. A cellular model of Holocene upland river basin
595 and alluvial fan evolution. Earth Surf. Process. Landforms 27, 269–288. doi:10.1002/esp.318

596 Coulthard, T.J., Neal, J.C., Bates, P.D., Ramirez, J., de Almeida, G. a M., Hancock, G.R., 2013.
597 Integrating the LISFLOOD-FP 2D hydrodynamic model with the CAESAR model: Implications for
598 modelling landscape evolution. Earth Surf. Process. Landforms 38, 1897–1906.
599 doi:10.1002/esp.3478

600 Coulthard, T.J., Ramirez, J., Fowler, H.J., Glenis, V., 2012. Using the UKCP09 probabilistic scenarios to
601 model the amplified impact of climate change on drainage basin sediment yield. Hydrol. Earth
602 Syst. Sci. 16, 4401–4416. doi:10.5194/hess-16-4401-2012

603 Coulthard, T.J., Van de Wiel, M.J., 2013. Climate, tectonics or morphology: what signals can we see in
604 drainage basin sediment yields? Earth Surf. Dyn. 1, 13–27. doi:10.5194/esurf-1-13-2013

605 Coulthard, T.J., Van De Wiel, M.J., 2007. Quantifying fluvial non linearity and finding self organized
606 criticality? Insights from simulations of river basin evolution. Geomorphology 91, 216–235.
607 doi:10.1016/j.geomorph.2007.04.011

608 Dotterweich, M., 2008. The history of soil erosion and fluvial deposits in small catchments of central
609 Europe: Deciphering the long-term interaction between humans and the environment — A
610 review. Geomorphology 101, 192–208. doi:10.1016/j.geomorph.2008.05.023

611 Einstein, H.A., 1950. The bed-load function for sediment transport in open channel flows, in:

612 Technical Bulletin No. 1026, USDA Soil Conservation Service. U.S. Department of Agriculture, p.
613 71.

614 Fryirs, K.A., Brierley, G.J., Preston, N.J., Kasai, M., 2007. Buffers, barriers and blankets: The
615 (dis)connectivity of catchment-scale sediment cascades. Catena 70, 49–67.
616 doi:10.1016/j.catena.2006.07.007

617 Harvey, A.M., 2002. Effective timescales of coupling within fluvial systems. Geomorphology 44, 175–
618 201. doi:10.1016/S0169-555X(01)00174-X

619 Harvey, A.M., 2001. Coupling between hillslopes and channels in upland fluvial systems: Implications
620 for landscape sensitivity, illustrated from the Howgill Fells, northwest England. Catena 42, 225–
621 250. doi:10.1016/S0341-8162(00)00139-9

622 Harvey, A.M., 1996. Holocene hillslope gulley systems in the Howgill Fells, Cumbria, in: Anderson,
623 M.G., Brooks, S.M. (Eds.), Advances in Hillslope Processes. John Wiley & Sons, Ltd, pp. 731–752.

624 Harvey, A.M., 1991. The influence of sediment supply on the channel morphology of upland streams:
625 Howgill Fells, Northwest England. Earth Surf. Process. Landforms 16, 675–684.
626 doi:10.1002/esp.3290160711

627 Harvey, A.M., Renwick, W.H., 1987. Holocene alluvial fan and terrace formation in the Bowland Fells,
628 Northwest England. Earth Surf. Process. Landforms 12, 249–257. doi:10.1002/esp.3290120304

629 Hooke, J.M., 2006. Human impacts on fluvial systems in the Mediterranean region. Geomorphology
630 79, 311–335. doi:10.1016/j.geomorph.2006.06.036

631 Houben, P., 2008. Scale linkage and contingency effects of field-scale and hillslope-scale controls of
632 long-term soil erosion: Anthropogeomorphic sediment flux in agricultural loess watersheds of
633 Southern Germany. GEOMORPHOLOGY 101, 172–191. doi:10.1016/j.geomorph.2008.06.007

634 Jerolmack, D.J., Paola, C., 2010. Shredding of environmental signals by sediment transport. Geophys.
635 Res. Lett. 37, 1–5. doi:10.1029/2010GL044638

636 Keesstra, S.D., van Dam, O., Verstraeten, G., van Huissteden, J., 2009. Changing sediment dynamics
637 due to natural reforestation in the Dragonja catchment, SW Slovenia. Catena 78, 60–71.
638 doi:10.1016/j.catena.2009.02.021

639 Lang, A., 2003. Phases of soil erosion-derived colluviation in the loess hills of South Germany. Catena
640 51, 209–221. doi:10.1016/S0341-8162(02)00166-2

641 Lexartza-Artza, I., Wainwright, J., 2009. Hydrological connectivity: Linking concepts with practical

642 implications. CATENA 79, 146–152. doi:10.1016/j.catena.2009.07.001

643 Liébault, F., Gomez, B., Page, M., Marden, M., Peacock, D., Richard, D., Trotter, C.M., 2005. Land-use
644 change, sediment production and channel response in upland regions. River Res. Appl. 21, 739–
645 756. doi:10.1002/rra.880

646 Macklin, M.G., Johnstone, E., Lewin, J., 2005. Pervasive and long-term forcing of Holocene river
647 instability and flooding in Great Britain by centennial-scale climate change. The Holocene 15,
648 937–943. doi:10.1191/0959683605hl867ft

649 Macklin, M.G., Jones, A.F., Lewin, J., 2010. River response to rapid Holocene environmental change:
650 evidence and explanation in British catchments. Quat. Sci. Rev. 29, 1555–1576.
651 doi:10.1016/j.quascirev.2009.06.010

652 Macklin, M.G., Lewin, J., 2003. River sediments, great floods and centennial-scale Holocene climate
653 change. J. Quat. Sci. 18, 101–105. doi:10.1002/jqs.751

654 Macklin, M.G., Lewin, J., 1993. Holocene river alluviation in Britain. Zeitschrift für Geomorphol.
655 Suppl. 88, 109–122.

656 Macklin, M.G., Lewin, J., Jones, A.F., 2014. Anthropogenic alluvium: An evidence-based meta-
657 analysis for the UK Holocene. Anthropocene 6, 26–38. doi:10.1016/j.ancene.2014.03.003

658 Macklin, M.G., Lewin, J., Woodward, J.C., 2012. The fluvial record of climate change. Philos. Trans. R.
659 Soc. A Math. Phys. Eng. Sci. 370, 2143–2172. doi:10.1098/rsta.2011.0608

660 Macklin, M.G., Passmore, D.G., Rumsby, B.T., 1992. Climatic and cultural signals in Holocene alluvial
661 sequences: the Tyne basin, northern England., in: Alluvial Archaeology in Britain. pp. 123–139.

662 Marden, M., Arnold, G., Gomez, B., Rowan, D., 2005. Pre- and post-reforestation gully development
663 in Mangatu Forest, East Coast, North Island, New Zealand. River Res. Appl. 21, 757–771.
664 doi:10.1002/rra.882

665 Michaelides, K., Chappell, A., 2009. Connectivity as a concept for characterising hydrological
666 behaviour. Hydrol. Process. doi:10.1002/hyp.7214

667 Schumm, S. a. (Colorado S., 1973. Geomorphic Thresholds and Complex Response of Drainage
668 Systems. Fluv. Geomorphol. doi:Doi 10.2307/622211

669 Simpson, G., Castelltort, S., 2012. Model shows that rivers transmit high-frequency climate cycles to
670 the sedimentary record. Geology 40, 1131–1134. doi:10.1130/G33451.1

671 Temme, A.J. a. M., Keiler, M., Karssenberg, D., Lang, A., 2015. Complexity and non-linearity in earth
672 surface processes - concepts, methods and applications. Earth Surf. Process. Landforms n/a–
673 n/a. doi:10.1002/esp.3712

674 Van De Wiel, M.J., Coulthard, T.J., 2010. Self-organized criticality in river basins: Challenging
675 sedimentary records of environmental change. Geology 38, 87–90. doi:10.1130/G30490.1

676 Van De Wiel, M.J., Coulthard, T.J., Macklin, M.G., Lewin, J., 2007. Embedding reach-scale fluvial
677 dynamics within the CAESAR cellular automaton landscape evolution model. Geomorphology
678 90, 283–301. doi:10.1016/j.geomorph.2006.10.024

679 Wainwright, J., Turnbull, L., Ibrahim, T.G., Lexartza-Artza, I., Thornton, S.F., Brazier, R.E., 2011.
680 Linking environmental regimes, space and time: Interpretations of structural and functional
681 connectivity. Geomorphology 126, 387–404. doi:10.1016/j.geomorph.2010.07.027

682 Walling, D.E., 1983. The sediment delivery problem. J. Hydrol. 65, 209–237. doi:10.1016/0022-
683 1694(83)90217-2

684 Ward, P.J., van Balen, R.T., Verstraeten, G., Renssen, H., Vandenberghe, J., 2009. The impact of land
685 use and climate change on late Holocene and future suspended sediment yield of the Meuse
686 catchment. Geomorphology 103, 389–400. doi:10.1016/j.geomorph.2008.07.006

687 Welsh, K.E., Dearing, J. a., Chiverrell, R.C., Coulthard, T.J., 2009. Testing a cellular modelling approach
688 to simulating late-Holocene sediment and water transfer from catchment to lake in the French
689 Alps since 1826. The Holocene 19, 785–798. doi:10.1177/0959683609105303

690 Wilcock, P.R.P., Crowe, J.J.C., 2003. Surface-based transport model for mixed-size sediment. J.
691 Hydraul. Eng. 129, 120–128. doi:10.1061/(ASCE)0733-9429(2003)129:2(120)

692